

Interfacial phenomena in nanocapacitors with multifunctional oxides Supplementary Information

I. STABILITY OF FERROELECTRIC STATE

We have calculated the energy of Pt/PZT/Pt capacitor in paraelectric (PE) state by constructing high symmetry PE state using linear approximation of the switching path from ferroelectric (FE) state to flipped polarisation FE state. Assuming that a state $S(t)$ is a configuration of a system in t state, where the states $t=0$ and $t=1$ correspond to FE states with opposite values of polarisation. We set up a PE state choosing parameter $t=0.5$ in the linear approximation:

$$S(t) = tS + (1-t)S.$$

Constructing a PE state for capacitors with both, Pt/PZT_{AO} and Pt/PZT_{BO₂} terminations, we calculated ζ as a difference between energy of FE state, E_{FE} , and PE state, E_{PE} , normalised on the thickness, n . The energy difference between FE and PE states, E_s , is the measure of stability of FE system. One can see that FE state is energetically advantageous to PE one for all thicknesses of PZT.

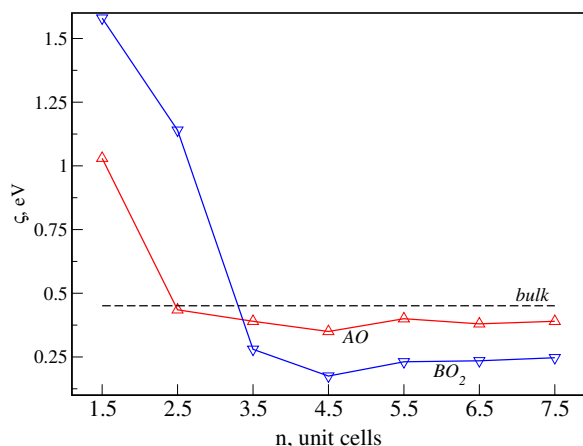


FIG. S1. The energy difference between PE and FE state in Pt/PZT capacitor with different PZT terminations. The value of ζ for bulk PZT is higher than that for thick Pt/PZT_{AO}/Pt and Pt/PZT_{BO₂}/Pt capacitors.

II. ELECTRONIC PROPERTIES OF THIN CAPACITORS

We found that Pt/PZT/Pt capacitors with $n_{crit} < 4.5$ u.c. of PZT exhibit metallic behaviour independently of termination. Fig. S2 shows the presence of populated electronic states at the Fermi level in the central layer of the system. The metallic states disappear when the thickness of the PZT is above the critical one.

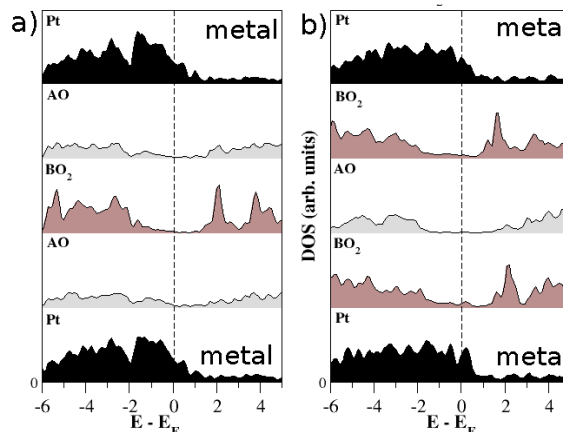


FIG. S2. Projected Density of States constructed for atomic layers for (a) Pt/PZT_{AO}/Pt and (b) Pt/PZT_{BO₂}/Pt capacitors for $n=1.5$ u.c. One can see that the central and interfacial layers of PZT are metallic.

III. CRYSTAL ORBITAL HAMILTON POPULATIONS (COHP) ANALYSIS

Crystal orbital Hamilton populations (COHP) analysis¹ has been performed using the SIESTA code², using the output interfacial configurations. The COHP separates the DOS into bonding, nonbonding, and antibonding contributions. For each pair of neighbouring atoms, the interaction between the ϕ_μ and ϕ_ν orbitals is described by the Hamiltonian matrix element $H_{\mu\nu} = \langle \phi_\mu | \hat{H} | \phi_\nu \rangle$. The product of the Hamiltonian matrix elements and the DOS matrix serves as a quantitative measure of the bond strength. The product either lowers (bonding) or raises (antibonding) the band-structure energy allowing to distinguishing between nature of bonding. Usually, the -COHP values are plotted so that bonding is characterised by positive values and antibonding by negative values.

The COHP analysis serves as a quantitative measure of the bond strength. The energy-resolved COHP plots allow distinguishing between bonding, nonbonding (no energetic effect), and antibonding contributions¹.

We have performed the partial crystal orbital Hamilton populations (COHP) analysis¹ for interfacial Pt and O species at P^+ and P^- interfaces of Pt/PZT with AO and BO₂ terminations. The COHP curves are shown in Fig. S6, where red and blue areas correspond to P^+ and P^- interfaces. The crossover at the Fermi energy separate positive (bonding) from negative values, indicating proper binding in the system. Since both interfacial layers are metallic, there is no gap separating occupied and unoccupied states as for central layers. COHP curved clearly shows bonding character of Pt-O bonds at P^+ interfaces. Although, the intensities of COHP curves for P^- of Pt/PZT_{AO} (Fig. S6a) is much lower than that for

Pt/PZT_{BO₂} (Fig. S6 b). The intensity of COHP curve indirectly suggests the strength of the bonding, identifying that Pt-O bonds at AO interfaces are much weaker than that at BO₂-terminated system. Moreover, the COHP curve at Fig. S6 shows a very weak, or even non-bonding character of Pt-O bonds at P⁻ interface.

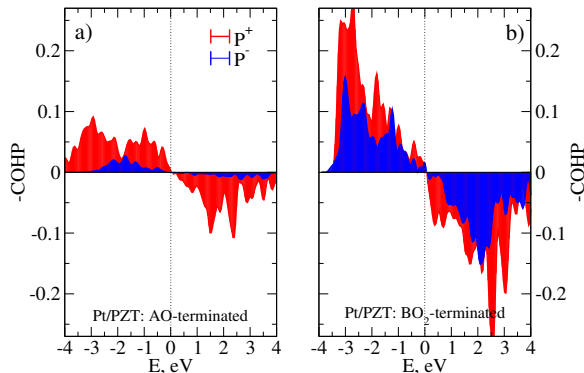


FIG. S3. The COHP analysis of interfacial Pt-O bonds at the P⁺ and P⁻ sides of a) Pt/PZT_{AO}/Pt, b) Pt/PZT_{BO₂}/Pt capacitors based on GGA WC calculations.

IV. CORRELATION EFFECTS

It is well known the failure of semilocal XC functionals to reproduce polaron formation in many condensed systems. This shortcoming can be traced to the self-interaction (SI) intrinsic to common semilocal approximations to the XC functional including the local density approximation (LDA) as well as the generalized gradient approximation (GGA). The importance of SI corrections in calculations based on semilocal XC functionals has been addressed more recently in terms of variation of the total energy with respect to fractional changes in the electronic occupations³. The DFT+U method, which was proposed to overcome this error, adds a Hubbard-like term to the total energy functional and solves it using the self-consistent field approach in the independent particle approximation. Correlation effects could be important especially for consideration of the systems with defects, the position of the defect levels in the gap, electron/hole localisation. In the current study we perform the calculations of idealised "clean" interfaces without the defects such as Oxygen vacancies, or Pb-cation deficiency, which are often presented in this type of systems.

While, GGA provides a good description of electronic and structural properties of metallic systems, the open gap oxide systems (as PZT) suffer from underestimated band gap. Wu and Cohen (WC) GGA functional used in this work is well known to reproduce structural properties of perovskite systems, and provides a good estimate of defect formation energies, while the value of the band gap is underestimated, although, to a known extent.

Indeed, the GGA WC functional (U=0) for studied P4mm phase predicts 2.8 eV, while the experimental value of the

band gap of bulk PZT is of 3.4-3.6 eV depending on the composition. We have performed calculations of electronic properties for bulk PZT with GGA+U using the value of U for *d* electrons of Ti and Zr of 8 eV, and 3 eV for *p* electrons of Oxygen species. The scissor operator within +U formalism shifts the position of the bottom of the conduction band (CB), thus, the band gap increases to 3.5 eV value (See Fig. S4 a, b). One can see that the valence band (VB) is formed by Oxygen 2*p* states, while the bottom of the conduction band (CB) is predominately formed by Ti 3*d* states, which is very similar to GGA prediction.

Since Pb is a heavy element and Pb-based semiconductors often pose a strong electron-phonon coupling, one can consider the effects of spin-orbit coupling (SOC) on the electronic structure. In that sense, PZT is a non-magnetic open band perovskite with a reasonably simple electronic structure characterised by Oxygen 2*p* states forming the top of VB, while Ti 3*d* states mostly contribute to the bottom of CB. Thus, the SOC in this system is expected to be minimal as shown in Fig. S4c, where electronic structure of bulk PZT demonstrates a minimal effect of applied SOC.

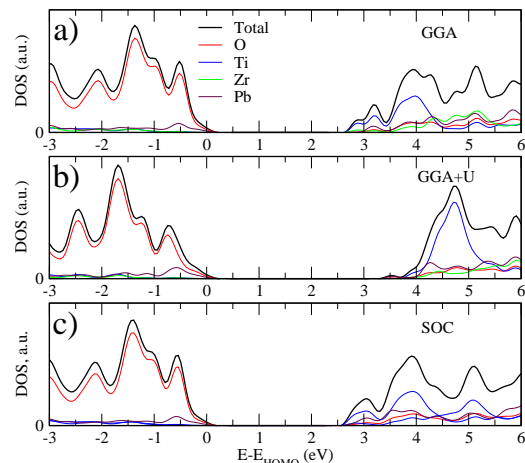


FIG. S4. The Density of States for bulk PZT calculated with a) WC GGA, b) GGA+U, and c) spin-orbit coupling effects.

To address the effect of correlation to screening properties we have constructed planar average electrostatic potential profiles for Pt/PZT_{AO}/Pt and Pt/PZT_{BO₂}/Pt nanocapacitors as well as profiles for freestanding AO- and BO₂-terminated slabs (See Fig. S5). The potential drop inside the ferroelectric (Δ_1) calculated with GGA+U is of 0.25 V and 0.23 V for AO- and BO₂-terminated slabs, respectively, which is systematically 0.12 V smaller than that predicted by GGA. Meanwhile, GGA and GGA+U predict very similar values of the asymptotic vacuum potential drop (Δ_2) with a difference of 0.01 V. We assume smaller values of the potential drop inside slabs is related to more localised nature of electrons treated

with GGA+U formalism. More importantly, in nanocapacitor geometry the AO-terminated system shows almost a flat profile of the electrostatic potential with $\Delta_3=0.011$ V, while BO_2 -terminated system shows the potential drop of 0.13 V, which is very similar to the values predicted by GGA (See for comparison Fig. 6).

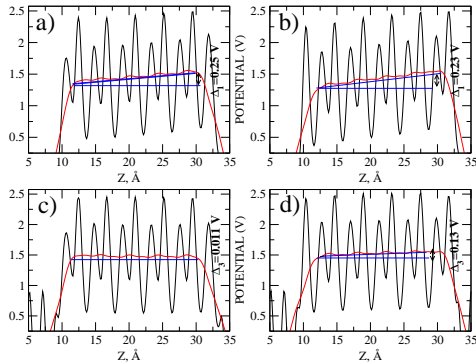


FIG. S5. Planar averaged electrostatic potential calculated with GGA+U in a) freestanding AO-terminated PZT slab; b) free-standing BO_2 -terminated PZT slab; c) Pt/PZT_{AO}/Pt and d) Pt/PZT_{BO₂}/Pt systems.

We have also found that the formation energies of the Pt/PZT interfaces calculated with GGA and GGA+U approached are very similar, with a few meVs difference per system. Thus, the inclusion of the correlation effects does not affect our conclusions on the chemical stability of PZT-based interfaces.

The analysis of COHP (See Fig. S6) shows a very similar picture to that predicted by GGA. Indeed, AO-terminated slab is characterised by weak Pt-O bonds at P^- interface, with a similar intensity of COHP curves calculated with GGA approach. Meanwhile, BO_2 -terminated interface shows qualitatively similar picture – with strong interfacial Pt-O bonds, while quantitatively, the intensity of COHP curves is higher in comparison to that calculated with GGA (See Fig. S3).

¹R. Dronskowski and P. E. Bloechl, “Crystal orbital Hamilton populations (COHP): energy-resolved visualization of chemical bonding in solids based on density-functional calculations,” *The Journal of Physical Chemistry* **97**(33), 8617 (1993).

²J. M. Soler, E. Artacho, J. D. Gale, A. García, J. Junquera, P. Ordejón, and D. Sánchez-Portal, “The SIESTA method for ab initio order-N materials simulation,” *Journal of Physics: Condensed Matter* **14**, 11 (2002).

³J. Varignon, M. Bibes, and A. Zunger, “Origin of band gaps in 3d perovskite oxides,” *Nature Communication* **10**, 1658 (2019).

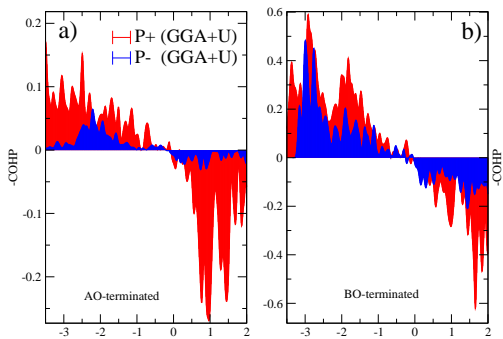


FIG. S6. The COHP analysis of interfacial Pt-O bonds at the P^+ and P^- sides of a) Pt/PZT_{AO}/Pt, b) Pt/PZT_{BO₂}/Pt capacitors based on GGA+U calculations shows a very similar behaviour to that observed with GGA (See Fig. S3).